Electronic structure and transport of Bi_2Te_3 and $BaBiTe_3$

P. Larson and S. D. Mahanti
Department of Physics and Astronomy, Michigan State University, East Lansing, Michigan 48824

M. G. Kanatzidis
Department of Chemistry, Michigan State University, East Lansing, Michigan 48824

(Received 10 September 1999)

We have carried out detailed *ab initio* electronic structure calculations of a novel thermoelectric compound $BaBiTe_3$ and its parent Bi_2Te_3, the best room-temperature thermoelectric known to date. The calculations were carried out using the self-consistent full-potential linearized augmented plane-wave method within density functional theory. The generalized gradient approximation of Perdew, Burke, and Ernzerhof was used to treat the exchange and correlation potential. For both systems, inclusion of spin-orbit interaction is crucial in understanding the gap structure near the Fermi energy. The calculated theoretical values of the gaps agree surprisingly well with experiment. A detailed comparison of the band structures of these two compounds indicates that the effective masses (expressed in units of free-electron mass) for both of them are highly anisotropic and comparable in magnitude. They lie in the range 0.01–0.4. The major difference between the two compounds is the large degeneracy of the band extrema in Bi_2Te_3, which is most likely the origin of its large thermoelectric figure of merit.

I. INTRODUCTION

There has been a recent revival of interest in developing a new generation of thermoelectric materials with a superior performance to the alloys of Bi_2Te_3, the currently available best thermoelectric.[1] As a result many promising new compounds are emerging and in order to better understand their thermoelectric (TE) properties one has to carefully examine their electronic structure. One such system, $BaBiTe_3$, like its parent compound Bi_2Te_3 is a narrow-gap semiconductor and has high thermoelectric power and low thermal conductivity, which are necessary for a good thermoelectric.[2,3] This compound consists of layers produced from segments of the Bi_2Te_3 structure separated by heavy Ba atoms between the layers. The underlying Bi/Te network substructure of $BaBiTe_3$ attempts to retain the high electrical conductivity and high thermoelectric power of Bi_2Te_3 while the heavy Ba^{2+} ions between these layers balance the anionic charge and tend to reduce the thermal conductivity of the phonons.[2,3]

Electronic structure calculations can serve an important role in determining which materials will prove useful for thermoelectric applications. The maximum efficiency (or coefficient of performance) of a heating (cooling) unit produced from thermoelectric materials depends on the dimensionless figure of merit *ZT*.

$$ZT = \sigma S^2 T/(\kappa_L + \kappa_e), \tag{1}$$

where S is the thermopower (Seebeck coefficient), σ is the electrical conductivity, κ_e is the electronic thermal conductivity, and κ_L is the lattice thermal conductivity (often much larger than κ_e in good thermoelectric materials).[4] It is believed that systems with many degenerate extrema, characterized by a degeneracy parameter γ, have higher thermoelectric power than those with a single extremum. This is because, for the same total carrier concentration, the concentration in each pocket is smaller for larger γ. This increases the value of S associated with each pocket compared to the value obtained for the single-band case because S increases with decreasing pocket carrier concentration. The amount of increase, however, depends on γ, the temperature, band gap, and other band parameters. If the carrier mobilities associated with each pocket are the same, then the total conductivity is independent of γ, but the conductivity-weighted thermopower for the multiband case is larger than for the single-band case.[5]

To see explicitly the effective mass dependence of the figure of merit we follow the arguments presented by Hicks and Dresselahaus.[6] They showed that in an anisotropic three-dimensional single-band case, when the thermal and electrical currents travel in the same direction (x), the figure of merit *ZT* increases with a parameter B which is defined by

$$B = \frac{1}{3\pi^2}\left(\frac{2k_BT}{\hbar^2}\right)^{3/2}(m_x m_y m_z)^{1/2}\frac{k_B^2 T\mu_x}{e\kappa_{\rm ph}}, \tag{2}$$

where m_i is the effective mass of the carriers (electrons or holes) in the ith direction, μ_x is the carrier mobility along the transport direction, and $\kappa_{\rm ph}$ is the lattice contribution to the thermal conductivity. In order to increase the value of Z, large effective masses, high carrier mobility, and low lattice thermal conductivity are necessary. Band structure calculations can directly give us information about the effective mass. It has been shown that semiconductors with a band gap of approximately $10k_BT$ best satisfy this criterion,[4] a property which can be easily determined from appropriate band structure calculations. In summary then, a detailed analysis of the electronic structure of a semiconducting compound can give information about the gap, the degeneracies of the

conduction and valence band extrema, and the effective mass parameters, all of which play an important role in determining Z.

In this paper we investigate in detail the electronic structures of Bi_2Te_3 and $BaBiTe_3$ from the point of view of thermoelectric properties. To understand the similarities and differences between $BaBiTe_3$ and Bi_2Te_3 it is important to make a careful comparison of their electronic structures. Whereas several calculations of the electronic structure of Bi_2Te_3 have been reported in the literature,[7–13] only one calculation on $BaBiTe_3$ has been reported[2] to our knowledge except for a brief report of our own work.[14] The previous electronic structure calculation[2] of $BaBiTe_3$ could not accurately determine the size of the gap, did not include spin-orbit interactions which proved essential for the calculation of the energy gap in Bi_2Te_3,[12,13] and did not investigate the effective masses associated with different band extrema in great detail. Also, there has been no detailed analysis using first-principles methods of how the inclusion of spin-orbit interaction alters the band structure near the Fermi energy in Bi_2Te_3 and how the bands rearrange to form a narrow-gap semiconductor. We address these questions here.

This paper is organized as follows. In Sec. II we describe briefly the method of electronic structure calculations and in Sec. III we give the results. In the results section the electronic structure of the parent compound Bi_2Te_3, will be discussed in detail first. This will help us isolate the important features characterizing a good thermoelectric and also test the adequacy of the currently available state of the art methods for obtaining electronic structures of narrow-gap semiconductors. Then the electronic structure of $BaBiTe_3$ will be presented and compared with that of Bi_2Te_3. These calculations will examine the nature of the bonding between Bi and Te p states and discuss the importance of spin-orbit interaction (SOI) in the gap formation. The calculated band gaps will be compared to experimental values. The effective masses associated with the band extrema will be evaluated and compared with available experimental values. Finally in Sec. IV we will give a brief summary and conclusions.

II. METHOD OF CALCULATION

Electronic structure calculations were performed using the self-consistent full-potential linearized augmented plane-wave method[15] (LAPW) within density functional theory (DFT),[16] using the generalized gradient approximation (GGA) of Perdew, Burke, and Ernzerhof[17] for the exchange and correlation potential. The calculations were performed using the WIEN97 package.[18] The values of the atomic radii were taken to be the same for all atoms, and each chosen so as to fill the space between the atoms. The chosen values are 2.9 a.u. for Bi_2Te_3 and 2.6 a.u. for $BaBiTe_3$, where a.u. is the atomic unit (0.52 Å). Adjustment of these parameters within a reasonable range showed little dependence on this variation. Convergence of the self-consistent iterations was performed for 44 **k** points for Bi_2Te_3 and 12 **k** points for $BaBiTe_3$ inside the reduced Brillouin zone to within 0.0001 Ry with a cutoff of -6.0 Ry between the valence and the core states. Scalar relativistic corrections were added for all systems studied and spin-orbit interaction was incorporated using a second variational procedure.[19]

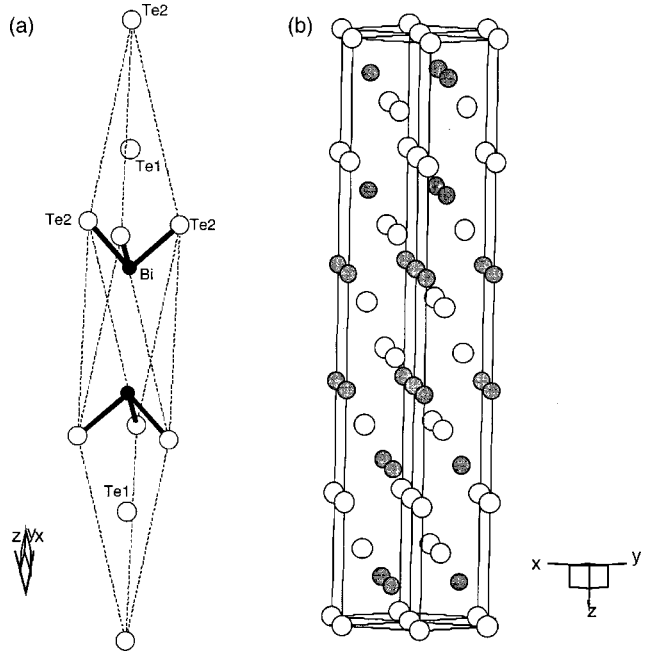

FIG. 1. Crystal structure of Bi_2Te_3: (a) Rhombohedral unit cell, (b) hexagonal unit cell. In (b) the Te atoms are open circles and Bi atoms are shaded circles.

III. RESULTS

A. Bi_2Te_3

Bi_2Te_3 and its alloys with Sb_2Te_3 and Bi_2Se_3 have served as the primary materials for thermoelectric devices for the past several decades.[20–22] As a result, there have been many electronic structure calculations performed on this material to understand its properties.[7–13] The importance of relativistic effects, especially that of the spin-orbit interaction, has been noted in each of these calculations. However, several questions remain to be resolved in the band structure of Bi_2Te_3. For example, Thomas *et al.*[12] explained the physics of the gap formation by incorporating the SOI, but were unable to incorporate it in their *ab initio* LAPW calculation. Later, Mishra *et al.*[13] did include SOI in their *ab initio* linear muffin-tin orbital (LMTO) calculation, but they did not explore the nature of the bands that hybridized (leading to uncrossing) near the Fermi energy. Further, none of the previous *ab initio* band structure calculations were successful in explaining the nature of both conduction band and valence band pockets in doped systems. Therefore we felt the need for further careful analysis of the detailed band structure of Bi_2Te_3.

The crystal structure of Bi_2Te_3 is rhombohedral with the space group D_{3d}^5 ($R\bar{3}m$) with five atoms in the unit cell.[23] Both the rhombohedral and hexagonal unit cells are shown next to each other in Figs. 1(a) and 1(b), respectively. Along the z direction (trigonal axis) it forms a five-atom layer (referred to as ''quintuple layer leaves'') with primarily ionic and covalent bonding within the layer, and Van der Waals bonding between the layers.[13,25] These five atoms reduce to three inequivalent atoms identified as Te1, Te2, and Bi in the figure. The corresponding Brillouin zone is given in Fig. 2.

The electronic structure of Bi_2Te_3 was calculated both with and without SOI. The band structure without SOI is

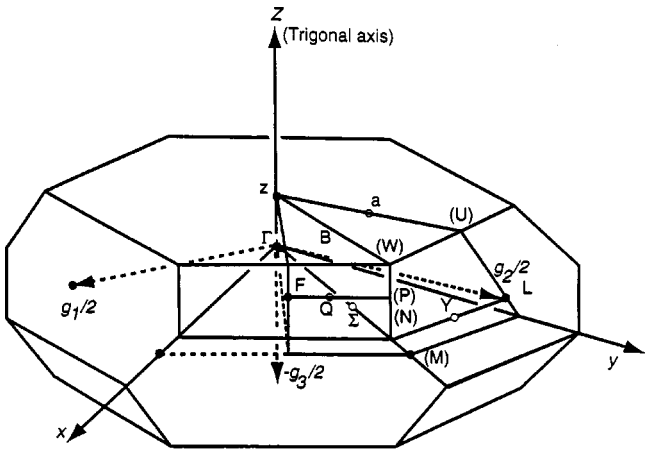

FIG. 2. Brillouin zone of Bi_2Te_3 (corresponding to the rhombohedral unit cell).

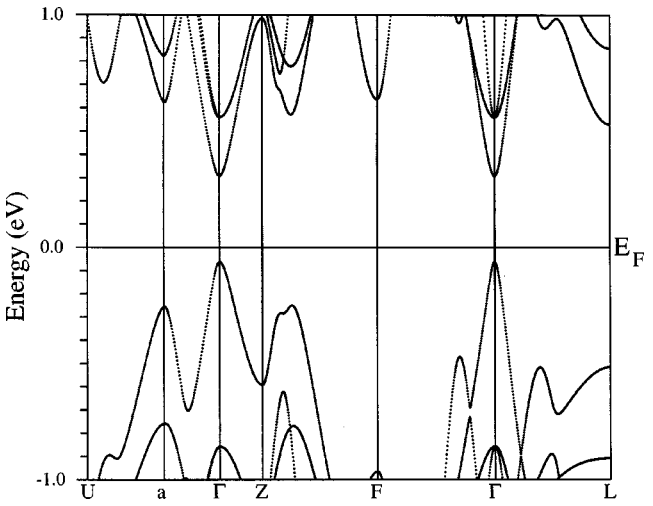

FIG. 3. Band structure of Bi_2Te_3 without spin-orbit interaction.

given in Fig. 3 which shows a direct band gap at the Γ point of about 0.37 eV. This is about twice the value reported by Thomas *et al.*,[12] who used the same LAPW method but a different local-density approximation (LDA) exchange-correlation potential. An orbital analysis reveals that the lowest conduction band (LCB) and the highest valence band (HVB) arise primarily from an admixture of Bi *p* and Te1 *p* bands. The conduction band is predominantly Bi *p* in nature whereas the valence band is predominantly Te1 *p*. Note that the Te1 atoms are in the layers that straddle the Van der Waals gap. Te2 *p* states lie primarily below the HVB although there is a small amount of Te2 *p* character in the HVB. In the *presence* of SOI the band structure near the Fermi energy is dramatically altered. The main effect of SOI is to move the conduction band bottom down relative to the top of the valence band (obtained without SOI) due to the different SOI's of Bi and Te so that the bottom of the conduction band crosses the top of the valence band at Γ. The resulting hybridization, which leads to uncrossing of the bands, opens a new gap which is indirect. This point was made by Thomas *et al.*[12] in their tight-binding parametrized calculations. They pointed out, however, the need for a complete self-consistent calculation including SOI to understand the subtle gap structure of Bi_2Te_3.

In Fig. 3 (band structure *without* SOI), we see that there are two additional peaks in the HVB (along Γa and ZF directions) and two valleys in the LCB (also along Γa and ZF directions) which have an energy slightly lower than the valence band maximum and slightly higher than the conduction band minimum, respectively. With SOI, the shapes of these peaks are virtually unchanged, but they move closer by approximately 0.50 eV. The strong hybridization occurring near Γ depresses the valence band peak to such an extent that the two valence band side peaks have now higher energy and they form the top of the valence band [Fig. 4(a)]. (This hybridization near the Γ point is much stronger than that for the side peaks in the valence and conduction bands so the overall shift of the bands is not rigid.) The two valence band maxima lie on the *yz* plane of the Brillouin zone, which is a plane of reflection symmetry. They will be denoted as $v1$ (along the Γa direction) and $v2$ (along the ZF direction). Similarly, the hybridization caused by the SOI shifts the conduction band minimum away from the Γ point to a point between Γ and Z [see Fig. 4(a)], which we will denote as $c0$. The net result is an indirect-gap semiconductor with a band gap of about 0.13 eV, in very good agreement with the previously published LMTO-ASA (atomic sphere approximation) calculation[13] of 0.11 eV. In addition to this minimum there are two higher-lying minima, $c1$ (along the Γa direction) and $c2$ (along the ZF direction). The direct gap between $v1$ and $c1$ is 0.27 eV and that between $v2$ and $c2$ is 0.23 eV.

Thomas *et al.* have carried out optical measurements in Bi-doped Bi_2Te_3 and find an indirect gap of 0.15 ± 0.02 eV and a direct gap of 0.22 ± 0.02 eV, which agree very well with the present calculations. Shubnikov–de Haas and de Haas–van Alphen measurements[24–27] of both *p*- and *n*-doped Bi_2Te_3 give sixfold degenerate valence and conduction band minima. The valence band maximum $v2$ appears to be the one seen in this experiment. The effective masses associated with both $v1$ and $v2$ along with their experimental values will be discussed in Sec. III D. In contrast to the valence band situation, the case for the conduction band is intriguing. The calculated minimum is along the ΓZ direction and is twofold degenerate. The next two higher minima $c1$ and $c2$ are both sixfold degenerate and are likely candidates to explain the cyclotron resonance measurement, which finds a sixfold-degenerate conduction band minimum.[28–32] The effective mass parameters associated with $c0$, $c1$, and $c2$, along with the experimental values, will also be discussed in Sec. III D. If the optical measurements[12] are correct, then the band structure results are amazingly good and the cyclotron resonance measurement is somehow missing the Fermi surface near the ΓZ axis. One has to investigate the reason for this more carefully. On the other hand, if they are not correct and the lowest gap is direct then the present band structure calculations are not accurate enough to reproduce this rather delicate gap structure near the Fermi energy in Bi_2Te_3. Below we discuss a possible scenario that can explain the observed sixfold-degenerate conduction band minimum. Also, careful angle-resolved photoemission measurements are currently being carried out by Liu and co-workers to obtain the band structure of both *n*- and *p*-doped Bi_2Te_3.[33] This will help to clarify the nature of the conduction band minimum.

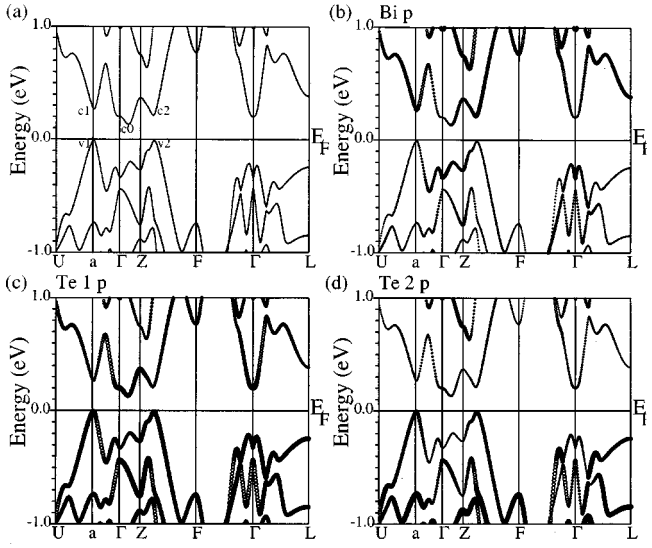

FIG. 4. Band structure of Bi_2Te_3 with spin-orbit interaction. Included are (a) total band structure, and orbital characters of the bands: (b) Bi p, (c) Te1 p, and (d) Te2 p. The sizes of the circles overlying the band structure are directly proportional to the strength of the orbital character.

As can be seen in Fig. 4(a), the $c2$ minimum is about 0.08 eV above the calculated absolute minimum $c0$ and the minimum $c1$ observed in cyclotron resonance measurements is about 0.15 eV above $c0$. Both $c1$ and $c2$ have sixfold degeneracy as seen in the experiment. As discussed above, the band structure near the Fermi energy depends sensitively on the spin-orbit-induced shifts in the LCB and HVB obtained in the absence of SOI. If this shift were larger by about 0.1–0.2 eV near the Γ point, then the minimum along the ΓZ direction could have shifted above the minimum along the ZF and Γa directions. Also it is possible that finite-temperature effects might interchange the minima. The net result would have been a sixfold-degenerate conduction band minimum as seen experimentally. A more accurate treatment of the spin-orbit interaction, which is the source of the subtle gap structure near the Fermi energy, has to be implemented, perhaps using a fully relativistic Dirac theory.

The orbital characters of the LCB and HVB in the *presence* of SOI are given in Figs. 4(b)–4(d), where the size of the circles that overlay the band structure plot are directly proportional to the strength of different orbital characters. The Bi p, Te1 p, and Te2 p bands are all involved in different amounts in the bonding near the Fermi level, but the LCB has a larger amount of Bi p character than Te1 p or Te2 p character, and the HVB has a larger Te1 p character than Bi p or Te2 p character. This can be seen by comparing the Bi p and Te1 p partial densities of states [Figs. 5(a)–5(d)] lying above and below the Fermi level. Te1 lies in the Van der Waals gap, bonded to one layer of Bi atoms below (or above) and weakly bonded to a Te1 atom across the gap, while Te2 is bonded to two layers of Bi atoms, one above and the other below. This results in the stabilization of the Te2 p bands which lie well below the Fermi level and do not play a significant role in transport. The n-type transport is primarily through Bi p orbitals (contributing to the lowest conduction band) and p-type transport through Te1 p orbitals (contributing to the highest valence band). This is consistent with the results of carrier scattering lifetime measurements[12] and with a previous calculation of electronegativity of each of the constituent atoms.[34] Finally, the Te1, Te2, and Bi valence s states lie approximately 10 eV below the Fermi energy and do not play any significant role in the bonding and transport properties.

B. $BaBiTe_3$

As discussed briefly in the introduction, $BaBiTe_3$ belongs to a class of compounds which are derived from the Bi_2Te_3 crystal structure.[2] The Bi/Te building blocks from Bi_2Te_3 are arranged side by side in layers connected by Te atoms. The heavy Ba atoms lie between the layers.[2,3,35] The structure of $BaBiTe_3$ also contains Te_2^{2-} units which serve to connect the Bi/Te blocks into layers. The crystal structure of $BaBiTe_3$ is more complicated than that of Bi_2Te_3 and has lower symmetry, orthorhombic rather than rhombohedral. The space group is $P2_12_12_1$ with 40 atoms in the unit cell,[2,3] but internal symmetries reduce the number of inequivalent atoms to ten:Ba1–2, Bi1–2, and Te1–6. The crystal structures of $BaBiTe_3$ and Bi_2Te_3 are projected onto the yz plane in Fig. 6, the underlying local Bi_2Te_3-like structures (shown by the shaded area) existing in $BaBiTe_3$ within regions connected by the Te5-Te6 chains. The Te2 and Te4 atoms lie on the edges of the layer and are bonded to only one layer of Bi atoms while the Te1 and Te3 atoms are bonded to two layers of Bi atoms. The Te1 atom has, however, a low Bi coordination and is likely to behave more like Te2 and Te4. In Bi_2Te_3, the Te1 atom is bonded to one layer of Bi atoms and lies near the Van der Waals gap, whereas the Te2 atom is bonded to two layers of Bi atoms. As a consequence the Te2 p bands in Bi_2Te_3 have a lower energy and appear away from the Fermi energy. Therefore, one would expect that in $BaBiTe_3$, Te1, Te2, and Te4 p bands would act more like the Te1 p bands in Bi_2Te_3, contributing to the valence band density of states near the Fermi energy, whereas Te3 p bands would act more as Te2 p in Bi_2Te_3, stabilized several eV below the Fermi with very little contribution to the density of states near the Fermi energy. Also, Bi p states will contribute primarily to the conduction band. Since Te5 and Te6 p states have no counterparts in Bi_2Te_3, the bands associated with these atoms will be new features in $BaBiTe_3$.

Electronic structure calculations were performed with and without spin-orbit interaction. The band structure of $BaBiTe_3$ is much more complicated than that of Bi_2Te_3 due to the larger number of atoms in the unit cell. We will focus, however, on the region close to the Fermi energy. Because of the geometry and the presence of Ba^{2+} ions, the orbital characters of the HVB and LCB in $BaBiTe_3$ are distinctly different from those seen in Bi_2Te_3. As a result the effect of SOI is not as dramatic. The Brillouin zone and the energy bands without SOI centered in the range of ~2 eV about the Fermi energy are given in Figs. 7 and 8, respectively. The top of the valence band occurs at a point between Γ and Z (this top valence band in the ΓZ direction is extremely flat) while the bottom of the conduction band lies at the Z point. The band gap at Z is calculated to be 0.45 eV, in good agreement (but see below for a discussion when SOI interaction is included) with the larger of the two band gaps found experimentally, 0.42 eV, but it cannot explain the smaller value of 0.28 eV

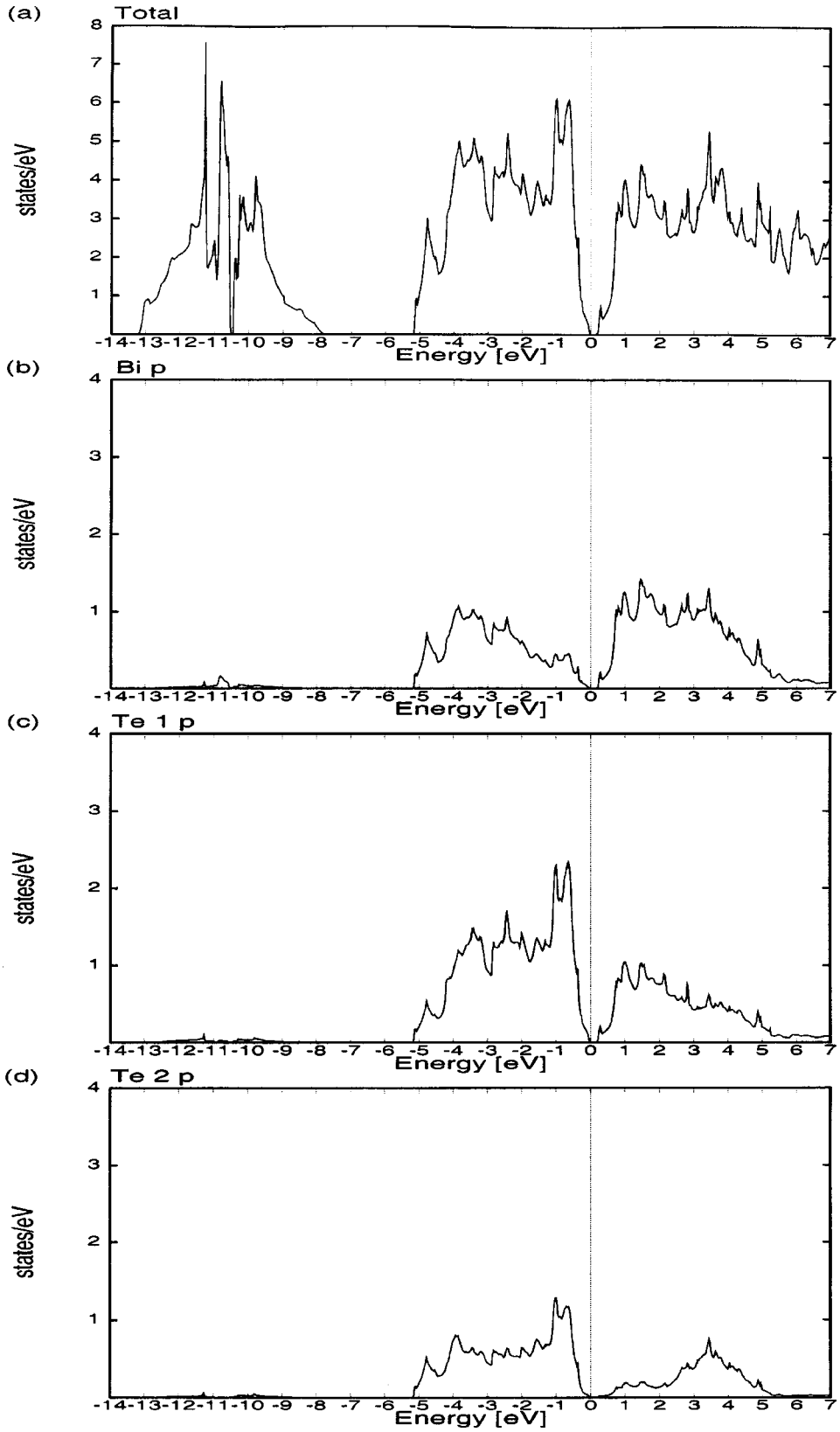

FIG. 5. Total and partial densities of states for Bi_2Te_3. Included are (a) total density of states, and partial density of states: (b) Bi p, (c) Te1 p, and (d) Te2 p.

also seen experimentally.[2] Our results agree with a previous unpublished LMTO calculation which did not include spin-orbit interaction.[36]

Introduction of SOI has some broad general effects, such as lifting the degeneracy of several bands and moving the conduction and valence bands closer together (see Fig. 9). However, it has little effect on the position of the top of the valence band of $BaBiTe_3$ while the bottom of the conduction band moves to a point between Γ and Z to form a gap which is very nearly ''direct.'' A careful analysis of our results

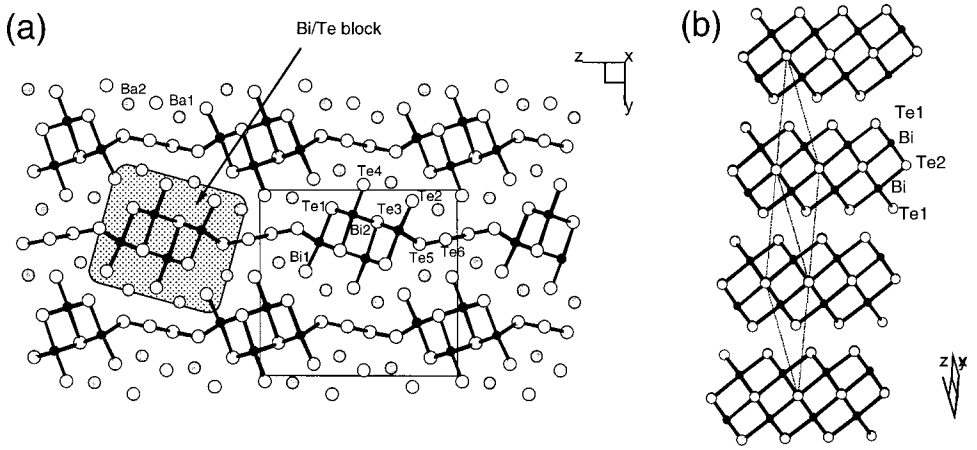

FIG. 6. Projection of the crystal structures in *yz* plane of (a) orthorhombic $BaBiTe_3$ and (b) rhombohedral Bi_2Te_3. The Bi/Te blocks are highlighted in the shaded area for $BaBiTe_3$.

shows that the top of the valence band is at (0, 0, 0.325) and the bottom of the conduction band is at (0, 0, 0.3625), in units of the primitive reciprocal lattice vectors $\mathbf{b}_1$, $\mathbf{b}_2$, $\mathbf{b}_3$. This new band gap is about 0.26 eV, in good agreement with the smaller experimental value of 0.28 eV.[2] There exist several other indirect band gaps in the spectrum, such as the 0.34 eV gap between the top of the valence band at Γ and the bottom of the conduction band between Γ and Δ. As pointed out before, the direct band gap at the Γ point is 0.47 eV, which is comparable to and may be identified with the larger of the experimentally observed band gaps of 0.42 eV.[2] The unusual shape of the experimental absorption spectrum near the threshold may result from the forbidden *p*-*p* transitions when $\Delta k = 0$. More accurate measurements and a detailed calculation of the optical absorption spectrum will clarify this issue.

The orbital characters of the bands in the neighborhood of the Fermi energy have been analyzed, but will not be shown to save space. It is observed that the main contribution near the bottom of the conduction band is associated with the Bi1 *p*, Te5 *p*, and Te6 *p* states while the Te1 *p*, Te2 *p*, and Te4 *p* states contribute most strongly to the top of the valence band. This is in agreement with the analogy made between the bonding found in Bi_2Te_3 and $BaBiTe_3$ with respect to the position of the atoms within the layers, and with the Te5 and Te6 atoms which contribute to the conduction band predominantly. The bands contributing to the density of states (DOS) near the Fermi energy consist of Te and Bi *p* bands, the Ba $5p$ bands lying about 13 eV below and the Ba $5d$ and $6s$ bands lying several eV above E_F. Therefore, the Ba $5p$, $5d$, and $6s$ orbitals contribute very little to the states near the Fermi level, the Ba^{2+} ion acting mainly as a spacer. The interesting case is that of Te5 and Te6 atoms, which connect the Bi/Te blocks together through the Te-Te chains along the *z* axis, and they have no analog in Bi_2Te_3. As pointed out above, the Te5 *p* and Te6 *p* states contribute to the bottom of the conduction band along with the Bi1 *p* and Bi2 *p* orbitals, primarily the former. This agrees with the ''lone pair'' ($2\sigma^*$) description of the Te5-Te6 states lying above the Fermi level.[2]

The nature of the charge transport in this material depends partly on the dispersion of the bands along different directions. As one can see, the dispersion along ΓY, perpendicular to the Ba^{2+} layers, is very small while that along ΓZ, i.e., through the Te5-Te6 ''necks,'' is appreciable. One also sees that there is a large dispersion in the $\Gamma\Delta$ direction which should be similar to that seen in the *xy* plane in Bi_2Te_3 (see

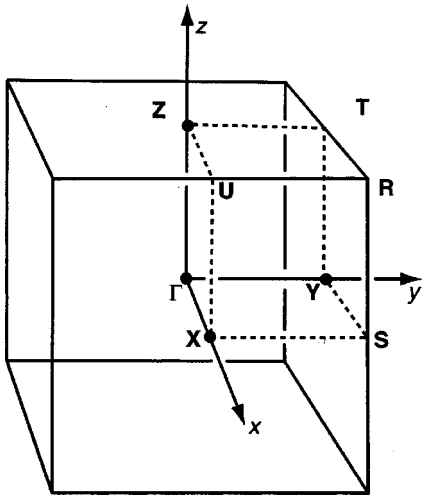

FIG. 7. Brillouin zone of $BaBiTe_3$.

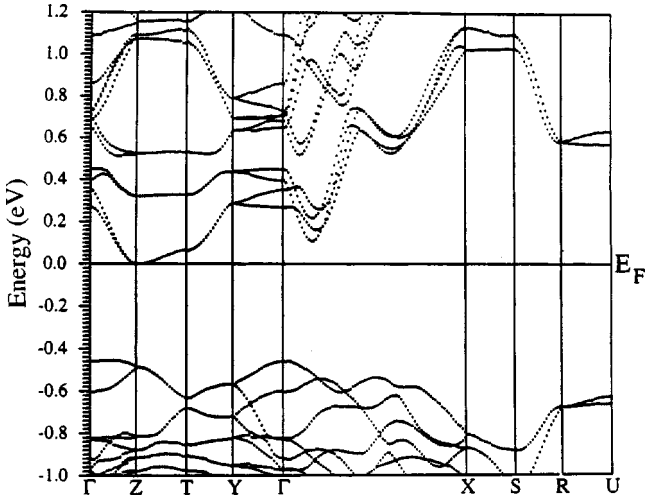

FIG. 8. Band structure of $BaBiTe_3$ without spin-orbit interaction.

Fig. 1). Thus $BaBiTe_3$ can be treated as a quasi-two-dimensional system with respect to charge transport.

Since the inclusion of SOI does not cause as drastic a change in the band structure as is the case for Bi_2Te_3, the position and the degeneracy of the conduction band minima calculated within the GGA are much more reliable in $BaBiTe_3$. However, several off-axis minima, whose energies lie above the bottom of the conduction band by about 0.1 eV, may contribute to the transport and increase the band degeneracy, thereby leading to a higher *ZT* value.

C. Comparison between Bi_2Te_3 and $BaBiTe_3$

Before we compare the band structure results for these two compounds we will briefly comment on the good agreement between the theoretical values of the gaps obtained using density functional theory (with the GGA approximation) and the experimental values. Although the values found for gaps in covalent semiconductors and insulators are usually underestimated in LDA/GGA,[37] the above agreement is quite gratifying. Orbital analysis of the bands near the gap region in both Bi_2Te_3 and $BaBiTe_3$ indicates that the gaps are caused by the hybridization of Bi *p* and Te *p* states. Since the gaps arise from hybridization rather than ionic or charge transfer (as in oxides) or strong covalent bonding (as in Si), it is possible that the LDA/GGA is better able to give a more realistic value of the gap in this system.

To determine the usefulness of $BaBiTe_3$ for room-temperature thermoelectric applications, comparisons should be made with Bi_2Te_3. Both Bi_2Te_3 and $BaBiTe_3$ contain band gaps of approximately $10k_BT$ at room temperature, a requirement for a good thermoelectric.[4] Also, since both materials have their HVB maxima and LCB minima lying off high-symmetry points, there will be a large degeneracy factor associated with these band extrema, which can lead to an enhancement of the thermoelectric coefficient. There are two features, however, which suggest that $BaBiTe_3$ may not be as good a thermoelectric material as Bi_2Te_3. Unlike the rhombohedral Bi_2Te_3, the lower symmetry of $BaBiTe_3$ means that the degeneracy factor γ associated with the band extrema, which enhances the thermopower, will be reduced.[5] Also, Bi_2Te_3 can be doped both *n*- and *p*-type for optimum thermoelectric properties. This is due to transport through the Bi channels for the electrons and transport through the Te1 channels for the holes. In $BaBiTe_3$, the blocks of Bi_2Te_3 structure are connected by Te5 and Te6 atom chains. Orbital analysis of the band structure calculation for $BaBiTe_3$ shows that they contribute significantly to the lowest conduction band along with the Bi atoms. Therefore, while electrons can flow through the layers, the Te5 and Te6 chains will block the holes from traveling through the Te1, Te2, and Te4 layers, so the hole mobility will be rather small. One hopes that the decrease of thermal conductivity due to the heavy Ba atoms lying between the Bi_2Te_3 layers may counteract part of these problems.[38,39]

D. Effective mass

As discussed in Eq. (2), the thermoelectric figure of merit *ZT* increases with the effective mass parameters of the carriers. It is therefore important to carefully examine these with a first-principles band structure calculation. The effective mass tensor is defined as[40]

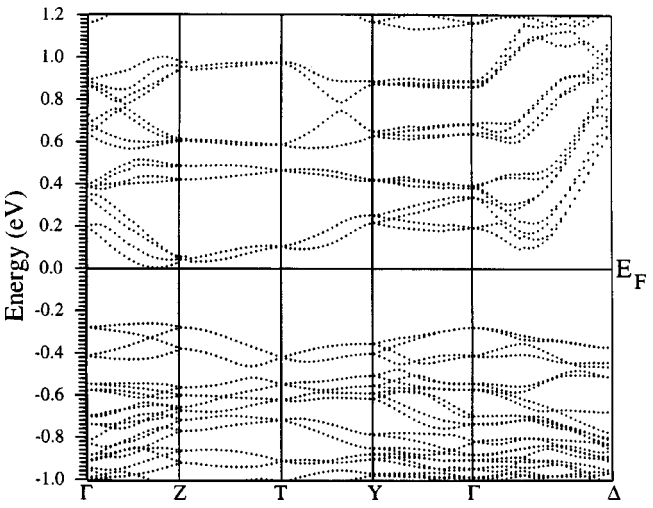

FIG. 9. Band structure of $BaBiTe_3$ with spin-orbit interaction.

$$[m]^{-1*}_{ij}=\alpha_{ij}=\hbar^{-2}\left[\frac{\partial^2 E}{\partial k_i \partial k_j}\right]. \tag{3}$$

In most cases, the off-diagonal terms of the mass tensor are small, so the diagonal elements of the mass tensor α_{ii} accurately give the inverse of effective mass parameters, m_{ii} (here $i=x,y,z$). In the general case, however, the mass tensor has to be diagonalized to obtain the effective masses associated with the principal directions. We fit the calculated *E* vs **k** along different orthogonal directions to parabolas and obtain the coefficients α_{ii}.

The effective masses for Bi_2Te_3 and $BaBiTe_3$ were obtained by calculating values of the energy close to different LCB minima and HVB maxima while moving along suitably chosen directions in the Brillouin zone. These values were then fitted to parabolas using the computer program[41] KALEIDAGRAPH (see Fig. 10). The energy dispersion curves near the LCB minima and HVB maxima of Bi_2Te_3 are known to display strong nonparabolic behavior,[24–28] but a fair approximation to a parabolic band can be made if points are chosen close to the band extrema.

Since all calculated extrema in Bi_2Te_3 lie on the plane of reflection symmetry (the *z* axis is the trigonal axis and the *y* axis is the bisectrix axis, and the *yz* plane is one of the three reflection planes) the energies near the top of the HVB and the bottom of the LCB can be fitted using the equation

$$2m_eE/\hbar^2=\alpha_{xx}k_x^2+\alpha_{yy}k_y^2+\alpha_{zz}k_z^2+2\alpha_{yz}k_yk_z, \tag{4}$$

where m_e is the free-electron mass and a constant term has been omitted. Note that the de Haas–van Alphen measurements find sixfold-degenerate hole and electron pockets lying on the reflection planes (containing the trigonal and bisectrix axes). The cross sections of these pockets in the *yz* plane are ellipses whose major axes make an angle θ with the *y* axis (the bisectrix axis). This angle θ is given by[24,26]

$$\theta=\tfrac{1}{2}\arctan[2\alpha_{yz}/(\alpha_{zz}-\alpha_{yy})]. \tag{5}$$

TABLE I. Theoretical and experimental values of effective mass tensor parameters associated with the conduction band minima and valence band maxima for Bi_2Te_3. The effective mass parameters are in units of the free-electron mass.

Conduction band	$c0$	$c1$	$c2$	Experiment (Ref. 24) ($\pm$10%)
$\alpha_{xx}=[m^{-1}]_{xx}$	20.25	112.75	95.84	46.9
$\alpha_{yy}=[m^{-1}]_{yy}$	3.97	2.87	3.56	5.92
$\alpha_{zz}=[m^{-1}]_{zz}$	3.75	5.49	6.20	9.50
$\alpha_{yz}=[m^{-1}]_{yz}$	2.93	2.54	2.39	4.22
θ	$-43.9°$	31.3°	32.7°	33.5°
Valence band		$v1$	$v2$	Experiment (Ref. 26) ($\pm$10%)
$\alpha_{xx}=[m^{-1}]_{xx}$		107.51	90.05	32.5
$\alpha_{yy}=[m^{-1}]_{yy}$		3.97	2.91	4.81
$\alpha_{zz}=[m^{-1}]_{zz}$		5.54	5.60	9.02
$\alpha_{yz}=[m^{-1}]_{yz}$		2.76	2.34	4.15
θ		37.1°	30.0°	31.5°

Theoretical values of the coefficients α_{ij} (which are the inverse of effective mass parameters) along with their experimental values are given in Table I. They agree quite well with the previous LMTO calculation.[42] The curvature in the x direction is obtained using values very close to the HVB maximum and LCB minimum and as we can see the theoretical values are about a factor of 3 too large compared to experiment. For higher doping, i.e., for larger k_x, the effective curvature decreases due to nonparabolic effects, and this improves the agreement with experimental values. However, the positions of the electron and hole pockets at $c1$, $c2$, $v1$, and $v2$ on the reflection planes as well as the angle θ associated with these pockets are accurately reproduced vis-a-vis experiment (see Table I and Fig. 11). The θ angle of the electron pocket associated with the $c0$ minimum is oriented at nearly 90° away from that seen in experiment. Therefore the $c0$ electron pocket either describes a real feature of the conduction band which has not been seen experimentally or is an artifact of the band structure calculation. The nature of this electron pocket must be examined both through fully relativistic band structure calculations and/or through further de Haas–van Alphen measurements of Bi_2Te_3 with a very small amount of n doping.

In $BaBiTe_3$, in spite of its more complicated crystal structure, the conduction and valence band extrema are relatively simple. They lie on the ΓZ direction and hence are twofold degenerate. Also due to the orthorhombic symmetry, the off-diagonal effective mass parameters are zero. Thus the principal axes of the electron and hole ellipsoids are oriented along the orthorhombic axes. The results are given in Table II. Since the arrangement of atoms along the x direction is quite similar in Bi_2Te_3 and $BaBiTe_3$, it is instructive to compare the corresponding effective masses. The effective masses along this direction are 0.09 (electrons) and 0.13 (holes) for the latter compared to about 0.01 in the former. Thus it appears that the geometry along the other two directions plays a significant role in the transport along the x axis. Whereas the effective mass parameters in the yz plane are comparable in Bi_2Te_3, they show substantial anisotropy in $BaBiTe_3$. The primary reason is the presence of Te5 and Te6 atoms in the latter. This is seen by examining the effective masses along the z axis (which traverses the Te5-Te6 chain; see Fig. 6). These are 0.08 (electrons) and 0.35 (holes). The small electron mass associated with the LCB which is of primarily Bi p character is due to a strong admixture of Te5 and Te6 p orbitals. In contrast, the HVB, which is composed primarily of Te1, 2, 4 and very little Te5, 6 p character, has a fourfold greater effective hole mass than the corresponding LCB electron mass.

From the results of experiments in Bi_2Te_3 and band calculations in both Bi_2Te_3 and $BaBiTe_3$, we note that the effective masses are rather small. Therefore it appears that the degeneracies of the HVB maxima and LCB minima, rather than large effective masses of the carriers, are responsible for

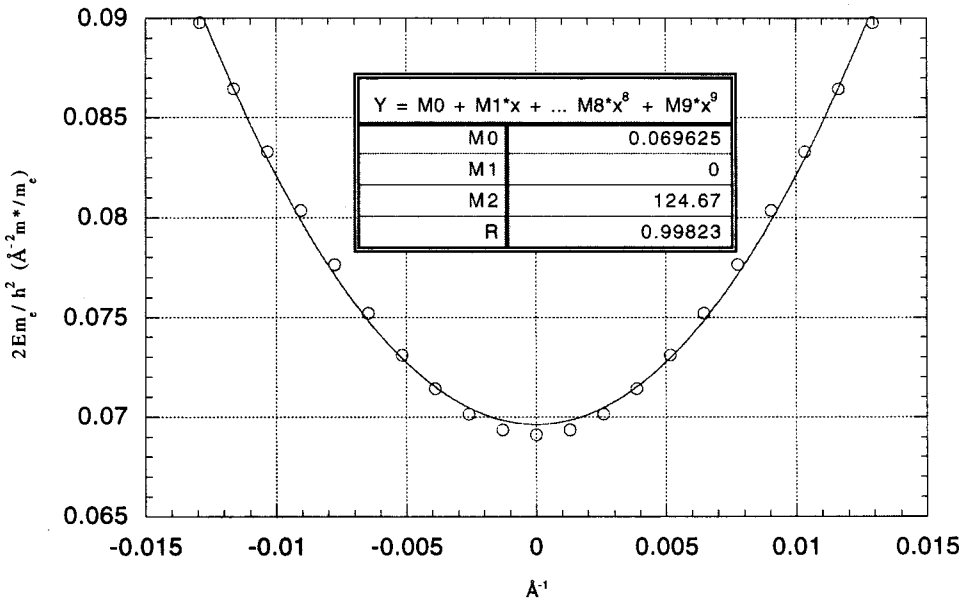

FIG. 10. Fitting of the energy band near the conduction band minimum to a parabola for Bi_2Te_3.

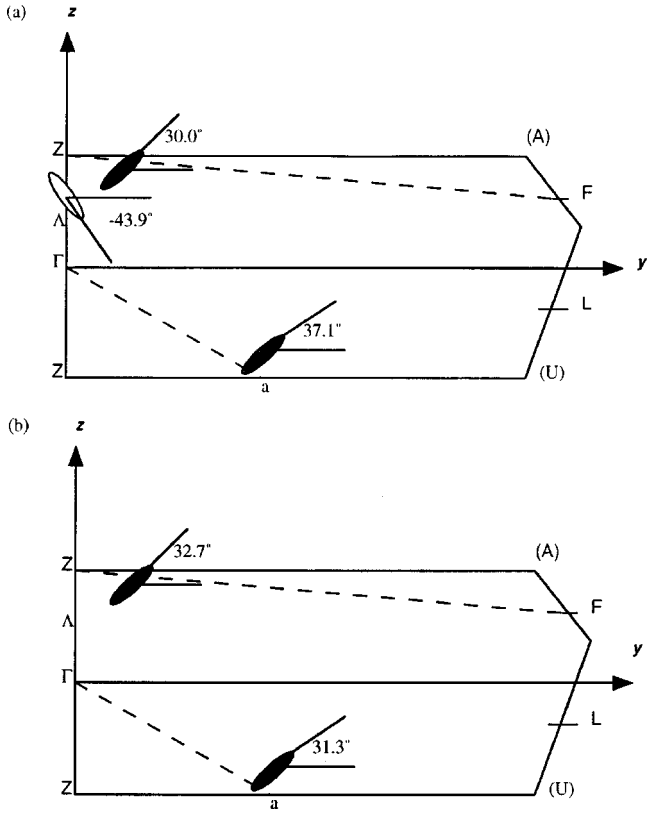

FIG. 11. Positions of the electron and hole pockets lying on the reflection plane of the Brillouin zone for Bi_2Te_3.

the observed high room-temperature ZT in Bi_2Te_3. A lower value of room-temperature ZT in $BaBiTe_3$ is consistent with a smaller degeneracy parameter γ. However, as we saw in the band structure calculation, there are several low-lying conduction band minima in $BaBiTe_3$ which with optimal n-type doping can give better ZT values.

IV. SUMMARY AND CONCLUSIONS

Electronic structure calculations were performed on both Bi_2Te_3 and $BaBiTe_3$ by applying full-potential LAPW and the generalized gradient approximation to density functional theory. Scalar relativistic and spin-orbit corrections were included in the calculation. The results for Bi_2Te_3 agree well with previous calculations using LMTO-ASA and the local density approximation to density functional theory.[13] We find that the electrons travel primarily through Bi channels while the holes travel primarily through channels produced by the Te1 atoms lying at the Van der Waals gap edge. The positions of the conduction band minima and valence band maxima result from a spin-orbit-induced nonrigid shift of the valence and conduction bands which cross; the resulting hybridization opens up a gap. While the calculated band gaps (indirect gap at 0.13 eV and direct gap of 0.23 eV) agree well with optical experiments,[12] and the sixfold-degenerate valence band maximum with Shubnikov–de Haas and de Haas–van Alphen measurements,[24,26] the situation of the conduction band minimum is less clear and needs further theoretical and experimental work.

TABLE II. Theoretical values of inverse effective mass parameters associated with the conduction band minimum and valence band maximum for $BaBiTe_3$. The effective mass parameters are in units of the free-electron mass.

Conduction band	ΓZ
$\alpha_{xx}=[m^{-1}]_{xx}$	11.61
$\alpha_{yy}=[m^{-1}]_{yy}$	2.79
$\alpha_{zz}=[m^{-1}]_{zz}$	13.16
Valence Band	ΓZ
$\alpha_{xx}=[m^{-1}]_{xx}$	7.61
$\alpha_{yy}=[m^{-1}]_{yy}$	5.40
$\alpha_{zz}=[m^{-1}]_{zz}$	2.89

Compared to Bi_2Te_3, very little work has been done on $BaBiTe_3$ to understand the nature of electron and hole pockets. The lowest band gap (0.27 eV) is indirect (nearly direct) and agrees with the experimental value.[2] The SOI, which played a crucial role in determining the nature of the gap in Bi_2Te_3, does not dramatically alter the gap structure in $BaBiTe_3$. Inclusion of SOI only lifts the degeneracy of the bands and reduces the size of the gap, but there is no band anticrossing and opening up of a new indirect gap as seen in Bi_2Te_3. Similarly, an orbital analysis of the bands suggests that the transport of holes will be through the Te atoms at the Van der Waals gap edge (denoted as Te1, Te2, and Te4), while the Bi atoms contribute to the electron transport along with Te5 and Te6 chains, which connect the Bi/Te regions together.

The above results suggest that attempts to optimize $BaBiTe_3$ as a p-type material should aim at preparing solid solutions of the type $BaBi_{1-x}Sb_xTe_3$, so that the Te sites are not disrupted. Given that the Te states predominate at the top of the HVB, Sb substitution at Bi sites should have minimal effects on the hole mobilities. Any substitution, however, at the Te sites (e.g., Se) is expected to greatly degrade the hole mobilities. On the other hand, attempts to optimize $BaBiTe_3$ as an n-type material are expected to be more challenging because the bottom of the conduction band has substantial contributions from both Bi states and Te states (Te5 and Te6). Therefore any substitution in either Bi or Te sites will likely have serious negative effects on the electron mobilities.

ACKNOWLEDGMENTS

We thank Dr. D. Y. Chung for helpful discussions. The work was partially supported by DARPA Grant No. DAAG55-97-1-0184.

[1] *Thermoelectric Materials—The Next Generation Materials for Small-Scale Refrigeration and Power Generation Applications*, edited by T. M. Tritt, M. G. Kanatzidis, G. D. Mahan, and H. B. Lyon, Jr., MRS Symposia Proceedings No. 545 (Materials Research Society, Pittsburgh, 1999).

[2] D. Y. Chung, S. Jobic, T. Hogan, C. R. Kannewurf, R. Brec, J. Rouxel, and M. G. Kanatzidis, J. Am. Chem. Soc. **119**, 2505 (1997).

[3] D. Y. Chung, T. Hogan, J. Schindler, L. Iordanidis, P. Brazis, C. R. Kannewurf, B. Chen, C. Uher, and M. G. Kanatzidis, in *Thermoelectric Materials—New Directions and Approaches*, edited by T. M. Tritt, M. G. Kanatzidis, H. B. Lyon, Jr., and G. D. Mahan, MRS Symposia Proceedings No. 478 (Materials Research Society, Pittsburgh, 1997), p. 333.

[4] G. Mahan, B. Sales, and J. Sharp, Phys. Today **50** (3), 42 (1997).

[5] This observation is in apparent disagreement with a statement made in a paper by Hicks and Dresselhaus (Ref. 6) where it is claimed that a one-band model always has higher thermopower than a two-band model where the two bands have thermopowers of the same sign. They did not incorporate the constraint on the total carrier density as we have done, however.

[6] L. D. Hicks and M. S. Dresselhaus, Phys. Rev. B **47**, 12 727 (1993).

[7] P. M. Lee and L. Pincherlee, Proc. Phys. Soc. London **81**, 461 (1963).

[8] F. Borghese and E. Donato, Nuovo Cimento Soc. Ital. Fis., B **53**, 283 (1968).

[9] Shin-ichi Katsuki, J. Phys. Soc. Jpn. **26**, 58 (1969).

[10] R. Togei and G. R. Miller, J. Phys. Chem. Solids Suppl. **32**, 349 (1971).

[11] E. V. Oleshko and V. N. Koryshin, Fiz. Tverd. Tela (Leningrad) **27**, 2856 (1985) [Sov. Phys. Solid State **27**, 1723 (1985)].

[12] G. A. Thomas, D. H. Rapke, R. B. Van Dover, L. F. Mattheis, W. A. Surden, L. F. Schneemaper, and J. V. Waszczak, Phys. Rev. B **46**, 1553 (1992).

[13] S. K. Mishra, S. Satpathy, and O. Jepsen, J. Phys.: Condens. Matter **91**, 461 (1997).

[14] S. D. Mahanti, P. Larson, D. Y. Chung, S. Sportouch, and M. G. Kanatzidis, in *Thermoelectric Materials–The Next Generation Materials for Small-Scale Refrigeration and Power Generation Applications*, edited by T. M. Tritt, M. G. Kanatzidis, G. D. Mahan, and H. B. Lyon, Jr., MRS Symposia Proceedings No. 545 (Materials Research Society, Pittsburgh, 1999), p. 23

[15] D. Singh, *Planewaves, Pseudopotentials, and the LAPW Method* (Kluwer Academic, Boston, 1994).

[16] P. Hohenberg and W. Kohn, Phys. Rev. **136**, B864 (1964); W. Kohn and L. Sham, *ibid.* **140**, A1133 (1965).

[17] J. P. Perdew, K. Burke, and M. Ernzerhof, Phys. Rev. Lett. **77**, 3865 (1996).

[18] P. Blaha, K. Schwarz, and J. Luitz, WIEN97 (Vienna University of Technology, Vienna, 1997).

[19] D. D. Koelling and B. Harmon, J. Phys. C **13**, 6147 (1980).

[20] H. J. Goldsmid, *Thermoelectric Refrigeration* (Plenum, New York, 1964).

[21] A. F. Ioffe, *Thermoelements and Thermoelectric Cooling* (Infosearch, London, 1957).

[22] D. M. Rowe, *CRC Handbook of Thermoelectrics* (CRC, Boca Raton, FL, 1995).

[23] R. W. G. Wyckoff, *Crystal Structures* (Krieger, Melbourne, FL, 1986), Vol. 2.

[24] H. Kohler, Phys. Status Solidi B **73**, 95 (1976).

[25] B. Schroeder, A. Von Middendorff, H. Kohler, and G. Landwehr, Phys. Status Solidi B **59**, 561 (1973).

[26] H. Kohler, Phys. Status Solidi B **74**, 591 (1976).

[27] S. A. Aliev, Sh. S. Ismailov, and I. G. Tagiev, Fiz. Tverd. Tela (St. Petersburg) **37**, 2851 (1995) [Phys. Solid State **37**, 1573 (1995)].

[28] O. S. Gryaznov, R. N. Ignat'ev, and B. Ya. Moizles, Fiz. Tekh. Poluprovodn. **17**, 1138 (1983) [Sov. Phys. Semicond. **17**, 716 (1983)].

[29] B. M. Gol'tsman, V. A. Kudinov, and I. A. Smirnov, *Semiconductor Thermoelectric Materials Based on Bi_2Te_3* (Nauka, Moscow, 1972).

[30] J. R. Drabble, R. D. Groves, and R. Wolfe, Proc. Phys. Soc. London **71**, 140 (1958).

[31] L. R. Testardi, P. J. Stiles, and E. Burstein, Solid State Commun. **1**, 28 (1963).

[32] R. B. Mallinson, J. A. Rayne, and R. W. Ure, Jr., Phys. Lett. **19**, 545 (1965).

[33] V. Jane and R. Liu (private communication).

[34] P. Pecheur and G. Toussaint, Phys. Lett. A **135**, 223 (1989).

[35] M. G. Kanatzidis, T. J. McCarthy, T. A. Tanzer, L. Chen, L. Iordanidis, T. Hogan, C. R. Kannewurf, C. Uher, and B. Chen, Chem. Mater. **8**, 1465 (1996).

[36] R. Brec and S. Jobic (unpublished).

[37] *Theory of the Inhomogeneous Electron Gas*, edited by S. Lundqvist and N. H. March (Plenum, New York, 1983), and references therein. In some systems, such as the half-Heusler compounds YNiSb and ZrNiSr, LDA/GGA overestimates the experimental band gap; see P. Larson, S. D. Mahanti, S. Sportouch, and M. G. Kanatzidis, Phys. Rev. B **59**, 15 660 (1999).

[38] R. R. Heikes and R. W. Ure, Jr., *Thermoelectricity: Science and Engineering* (Interscience, New York, 1961).

[39] T. C. Harman and J. M. Honig, *Thermoelectric and Thermomagnetic Effects and Applications* (McGraw-Hill, New York, 1967).

[40] N. W. Ashcroft and N. D. Mermin, *Solid State Physics* (Harcourt Brace College Publishers, New York, 1976), p. 228.

[41] KALEIDAGRAPH (Synergy Software, Inc., Reading, PA, 1999).

[42] Using the values of α_{ij} provided in Ref. 13, the angle θ would be approximately 40°, not 35° as reported in their paper.